Appl. Math. J. Chinese Univ.
2025, 40(1): 223-237

Chirped solutions and dynamical properties of the resonant Schrödinger equation with quadratic-cubic nonlinearity

TANG Jia-xuan

Abstract. In this paper, the nonlinear Schrödinger equation combining quadratic-cubic nonlinearity is considered, which can be represented by an approximate model of relatively dense quasi-one-dimensional Bose-Einstein condensate. Based on the bifurcation theory, we proved the existence of solitary and periodic solutions. The methods we take are the trial equation method and the complete discrimination system for polynomial method. Therefore, we obtain the exact chirped solutions, which are more abundant in type and quantity than the existing results, so that the equation has more profound physical significance. These two methods are rigorously mathematical derivation and calculations, rather than based on certain conditional assumptions. In addition, we give some specific parameters to graphing the motion of the solutions, which helps to understand the propagation of nonlinear waves in fiber optic systems.

§1 Introduction

Nonlinear science is involved in optical fiber, communications and more, scholars use nonlinear partial differential equations to build mathematical models and mathematical physical knowledge to describe some nonlinear phenomena[1]. The nonlinear Schrödinger equation (NLSE) is one of the common nonlinear partial differential equations, which describes the modulation equation for nonlinear waves and covers almost all branches of physics. For example, Bose-Einstein condensation(BEC), superconductivity and superfluidity, optical soliton communication, soliton lasers and optical waveguides in nonlinear optics[2-5]. In nonlinear optics, conditions based on a balance between group velocity dispersion (GVD) and self-phase modulation (SPM) allow optical solitons to propagate over long distances in uniformly nonlinear fiber without amplitude attenuation or shape change[6]. However, for the propagation of subpicosecond and femtosecond pulses in fibres, not only GVD and SPM but also higher order terms

Received: 2023-12-06. Revised: 2024-02-29.
MR Subject Classification: 35Q55.
Keywords: chirped solutions, bifurcation theory, trial equation method, quadratic-cubic nonlinearity, nonlinear waves.
Digital Object Identifier(DOI): https://doi.org/10.1007/s11766-025-5127-7.

such as third and fourth-order dispersions, self-steepening and Raman self-frequency need to be considered[7,8]. In recent years, the quadratic and cubic nonlinearities in the field of nonlinear optics have received special attention[9]. The nonlinear Schrödinger equation, which incorporates both quadratic and cubic nonlinearities, is often employed as an approximate model for describing the dynamics of a relatively dense quasi-one-dimensional BEC. This equation can be derived by considering the interplay of attractive and repulsive interactions between atoms in the BEC, allowing for a more comprehensive representation of the behavior of condensates compared to a standard NLSE with only quadratic nonlinearity. The inclusion of cubic nonlinearity allows for a more accurate description of certain physical phenomena in such systems[10,11]. The resonant NLSE with quadratic-cubic nonlinearity studied in this paper plays a very important role in describing the phenomenon of analogue pulse propagation in optical fiber[12-15], the governing resonant NLSE, for quadratic and cubic nonlinearities, with perturbation terms that is studied in nonlinear optics is given in its dimensionless form as:

$$\begin{gathered} ih_t+a_1h_{xx}h+a_2\frac{|h|_{xx}}{h}h+\Big(a_3\,|h|+a_4|h|^2\Big)\,h=i\alpha h_x \\ +i\lambda\Big(|h|^{2m}h\Big)_x+i\theta_1\Big(|h|^{2m}\Big)_x h+i\theta_2|h|^{2m}h_x+\sigma\frac{h^*_{xx}}{|h|^2}h^2, \end{gathered} \tag{1}$$

where $h(x,t)$ shows the wave profile of complex valued with $i=\sqrt{-1}$. x, t denote time and space variables respectively. a_1 and a_2 are the group velocity dispersion and Boham potential for chiral solitons with quantum hall cause respectively. The terms a_3 and a_4 are quadratic-cubic nonlinear together. The α indicates inter-model dispersion, also λ illustrates self-steepening having short pulses, while θ_1 and θ_2 are associated with nonlinear dispersions. The parameter m is the full nonlinearity. Biswas et al. applied the semi-inverse variational principle to retrieve the solitary solutions of Eq.(1)[16]. Seadawy et al. achieved optical solitons and solitary waves solutions of Eq.(1) by employing F-expansion method[17]. One of the new developments in this paper is the adoption of chirped wave transformation, which is more common than linear transformation.

Research has shown the importance of chirped pulses in pulse compression and amplification, and scholars have conducted numerous experiments with chirped pulses to demonstrate their irreplaceable role in the design of optical fiber amplifier and solitary waves-based communications[18-21]. Moreover, based on the wide application of chirped pulse amplification techniques in optics and dynamics, the study of chirped solutions has important theoretical significance and application value[22-25]. Therefore, it is particularly important to explore the applications of solutions of NLSE, especially exact chirped solutions and traveling wave solutions, where we can analyze and interpret various nonlinear physical phenomena[26-29]. Mecelti et al. investigated chirped self-similar waves for NLSE [30]. Zhou et al. applied a direct method to conduct chirp waves of higher-order NLSE [31]. Arshed used the $\left(\frac{G'}{G^2}\right)$-expansion technique and an equivalent form for the $(\exp(-\phi(\xi)))$-expansion technique to extract new exact solutions of the resonant fractional NLSE [32]. Bulut et al. structured an extended sinh-Gordon equation expansion method to construct various optical solitions of the nonlinear resonant Schrödinger equation with space-time dispersion and intermodal dispersion [33]. Rezazadeh et al. studied the optical solition of the generalized non-autonomous NLSE by using the new Kudryashov method (NKM) and tested the above model with a time correlation coefficient[34]. Mustafa et al. derived dark, bright, dark-bright or combined optical solition and singular solition based on three nonlinear dielectric fibers with the sine-Gordon equation method (SGEM)[35].

With the study of nonlinear development equations and the flexible use of methods such as SGEM, NKM and SVP, many types of solutions have been solved. In addition, there are many ways to solve the exact solutions of the nonlinear partial differential equations, such as Kudryashov method[36], generalized auxiliary equation technique[37], fractional Iteration algorithm [38,39], Variational Iteration algorithm-I [40,41], Variational iteration algorithm-II[42,43], Riccatti transformation method [44], meshless techniques[45,46], modified $\left(\frac{G'}{G^2}\right)$-expansion method[47]. By using these methods, exact solutions whose type are Jacobi elliptic, singular periodic, kink wave, algebraic soliton can be obtained. The approaches used in this paper are the trial equation method[48-52] and the complete discrimination for polynomial method[53-54], which are widely used in the field of exact solution solving, and systematically provide all the classifications of solutions, including solitary waves, rational functions, Jacobi elliptic functions, and trigonometric functions. As long as the parameters are given, we can know what the form and type of the solutions are and which are stable or unstable[48-55]. However, these methods can only achieve single traveling wave solutions, not obtain multiple solitary solutions. Further research is needed to improve the limitations of these approaches.

The full text is organized as follows. In Section 2, the equation is converted into integral form by using the trial equation method. In Section 3, based on the bifurcation method, the existence of different types of solutions is proved. In Section 4, the chirped solutions are obtained with the complete discrimination for polynomial method. In Section 5, some graphs of the solutions are given to help understand the physical interpretation of the model. In the last section, we give the conclusion.

§2 Trial equation method

Considering chirped transform, we substitute Eq.(2) into the Eq.(1)

$$h\left(x,t\right)=\rho\left(\xi\right)e^{i(\chi(\xi)-kx)},\xi=t-ux, \tag{2}$$

where $u=\frac{1}{v}$, v expresses speed, k is the wave number, then we derive the real part

$$\begin{aligned}&u^2\left(a_1+a_2-\sigma\right)\rho^{''}+(-1-2kua_1+\alpha u-2\sigma ku)\rho\chi^{'}\\&+u^2(-a_1-\sigma)\rho\left(\chi^{'}\right)^2+k\left(-a_1k+\alpha-\sigma k\right)\rho+a_3\rho^2+a_4\rho^3\\&+u\left(\lambda+\theta_2\right)\rho^{2m+1}\chi^{'}++k\left(\lambda+\theta_2\right)\rho^{2m+1}=0,\end{aligned} \tag{3}$$

and the imaginary part

$$\begin{aligned}&(1+2a_1ku+\alpha u+2\sigma ku)\,\rho^{'}+2u^2(a_1+\sigma)\rho^{'}\chi^{'}+u^2(a_1+\sigma)\rho\chi^{''}\\&+u[\lambda(2m+1)+2m\theta_1+\theta_2]\rho^{'}\rho^{2m}=0.\end{aligned} \tag{4}$$

Integration of the imaginary part gives

$$\chi^{'}=\frac{c}{u^2\left(a_1+\sigma\right)}\rho^{-2}-\frac{\lambda(2m+1)+2m\theta_1+\theta_2}{u\left(a_1+\sigma\right)}\rho^{2m}-\frac{1+2a_1ku+\alpha u+2ku\sigma}{2u^2\left(a_1+\sigma\right)}. \tag{5}$$

Substituting Eq.(5)into the real part, we get

$$\begin{aligned}
&u^2(a_1+a_2-\sigma)\rho''-\tfrac{(\lambda+\theta_2)(2\lambda m+\lambda+2m\theta_1+\theta_2)}{a_1+\sigma}\rho^{4m+1}\\
&+\left[k\left(\lambda+\theta_2\right)-\tfrac{4\alpha u^2(2\lambda m+\lambda+2m\theta_1+\theta_2)+(1+2a_1ku+\alpha u+2k\sigma u)}{2u^2(a_1+\sigma)}\right]\rho^{2m+1}\\
&+\left[k(-a_1k+\alpha-\sigma k)+\tfrac{(1+2a_1ku+\alpha u+2k\sigma u)(1+2a_1ku-3\alpha u+2k\sigma u)}{4u^2(a_1+\sigma)}\right]\rho\\
&+\left[\tfrac{c(\lambda+\theta_2)}{u(a_1+\sigma)}+2cu(2\lambda m+\lambda+2m\theta_1+\theta_2)\right]\rho^{2m-1}\\
&-c^2\rho^{-3}+a_3\rho^2+a_4\rho^3=0
\end{aligned}\tag{6}$$

For ρ, Eq.(6)is not integrable. Therefore, the trial equation method is used to convert it into an integral form. We assume that the trial equation is

$$\rho''=\sum_{i=1}^{n}b_i\rho^i.\tag{7}$$

Substitute Eq.(7) into Eq.(6), then using the principle of equilibrium we can arrive at $m=\frac{1}{2}$, $n=3$, Eq.(7) can be written as the following

$$\rho''=b_3\rho^3+b_2\rho^2+b_1\rho+b_0,\tag{8}$$

where

$$\begin{aligned}
b_3&=\tfrac{-2a_4(a_1+\sigma)+[\lambda(2m+1)+2m\theta_1+\theta_2](\lambda+\theta_2)}{2u^2(a_1+a_2-\sigma)(a_1+\sigma)},\\
b_2&=\tfrac{-2u^2(a_1+\sigma)[a_3+k(\lambda+\theta_2)]+4\alpha u^2[\lambda(2m+1)+2m\theta_1+\theta_2]+(1+2a_1ku+\alpha u+2\sigma ku)}{2u^4(a_1+a_2-\sigma)(a_1+\sigma)},\\
b_1&=\tfrac{4u^2k(a_1k-\alpha+\sigma k)(a_1+\sigma)-(1+2a_1ku+\alpha u+2\sigma ku)(1+2a_1ku-3\alpha u+2\sigma ku)}{4u^4(a_1+a_2-\sigma)(a_1+\sigma)},\\
b_0&=\tfrac{-2cu^2(a_1+\sigma)[\lambda(2m+1)+2m\theta_1+\theta_2]-c(\lambda+\theta_2)}{u^3(a_1+a_2-\sigma)(a_1+\sigma)}.
\end{aligned}\tag{9}$$

Integrating both sides of Eq.(8) by multiplying by ρ', and make $\kappa=\rho+\frac{b_2}{3b_3}$.

$$(\rho')^2=c_4\rho^4+c_3\rho^2+c_2\rho+c_1,\tag{10}$$

where

$$\begin{aligned}
c_4&=\tfrac{b_3}{2},\\
c_3&=\tfrac{3b_1b_3-b_2^2}{3b_3},\\
c_2&=\tfrac{4b_2^3+12b_1b_2b_3+36b_3^2b_0}{18b_3^2},\\
c_1&=\tfrac{-3b_2^4-18b_2^2b_1b_3}{162b_3^3}-\tfrac{2b_1b_2+6b_3^2c_0}{3b_3}.
\end{aligned}\tag{11}$$

§3 Qualitative studies to Eq. (10)

Based on the bifurcation theory, we can analyze Eq.(10). It is transformed into a two-dimensional dynamical system.

$$\begin{cases}\frac{d\rho}{d\xi}=q,\\ \frac{dq}{d\xi}=2c_4(\rho^3+\eta_1\rho+\eta_2),\end{cases}\tag{12}$$

where $\eta_1=\frac{c_3}{2c_4}$, $\eta_2=\frac{c_2}{4c_4}$. The following Hamiltonian function can represent its total energy.

$$H(\rho,q)=\frac{q^2}{2}-\frac{1}{2}(c_4\rho^4+c_3\rho^2+c_2\rho+c_1),\tag{13}$$

where ρ represents generalized momentum and q represents generalized coordinates. We consider the Eq. (10) to be conservative, therefore the trajectory is located on the contour line of $H(\rho,q)=D$, where D is a constant.

The potential energy formula can be expressed as

$$I(\rho) = -\frac{1}{2}(c_4\rho^4 + c_3\rho^2 + c_2\rho + c_1). \tag{14}$$

We discuss the root of $I'(\rho)$ in order to analyze the dynamical properties of Eq.(9)

$$I'(\rho) = -2c_4(\rho^3 + \eta_1\rho + \eta_2), \tag{15}$$

its complete discrimination system is as follows

$$\Delta = -(27\eta_2^3 + 4\eta_1^3). \tag{16}$$

Scenario 1. $\Delta = 0$, $\eta_1 < 0$, then $I^{'}(\rho) = -2c_4(\rho - \alpha_1)(\rho - \alpha_2)^2$, and $\alpha_1 + 2\alpha_2 = 0$.

If $c_4 < 0$, the center is $(\alpha_1, 0)$. If $c_4 > 0$, the saddle point and cusp are $(\alpha_1, 0)$ and $(\alpha_2, 0)$. When $c_4 = -1$, $\eta_1 = -3$, $\eta_2 = 2$, then $(-2, 0)$ is a center, (1,0) is called cusp. We see in Fig.1, the nonlinear periodic trajectory is a closed curve in blue, which indicates the existence of periodic solutions, and the nonlinear homoclinic trajectory is represented by a red curve, corresponding to a bell-shaped solitary solution. The black curve represents the the supernonlinear periodic trajectories.

Scenario 2. $\Delta < 0$, then$I^{'}(\rho) = -2c_4(\rho - \alpha_1)[(\rho - \alpha_2)^2 + \alpha_3{}^2]$.

At this point, $(\alpha_1, 0)$ is a center. When $c_4 = -1$, $\eta_1 = -2$, $\eta_2 = -4$, then $(2, 0)$ is a center. We see in Fig.2, the black closed curve containing the center point is the nonlinear periodic trajectory, which denotes the existence of periodic solutions.

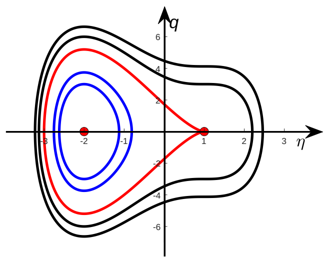

Figure 1. Corresponding phase portrait of Scenario 1.

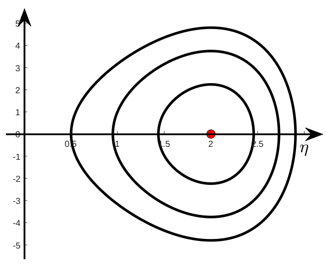

Figure 2. Corresponding phase portrait of Scenario 2.

Scenario 3. $\Delta = 0$, $\eta_1 = 0$, then $I^{'}(v) = -2c_4\rho^3$.

Which (0,0) is a center, this situation is similar to Scenario 2, so we will only discuss one of them.

Scenario 4. $\Delta > 0$, $\eta_1 < 0$, then $I^{'}(\rho) = -2c_4(\rho - \alpha_1)(\rho - \alpha_2)(\rho - \alpha_3)$, $\alpha_1 + \alpha_2 + \alpha_3 = 0$, and $\alpha_1 > \alpha_2 > \alpha_3$.

If $\eta_2 \neq 0$ the global phase portrait for this Scenario 4 is asymmetric, we discuss the case where when $\eta_2 = 0$, the phase portrait is symmetrical. When $c_4 = -1$, $\eta_1 = -3$, $\eta_2 = 0$, $\left(\sqrt{3}, 0\right)$, $\left(-\sqrt{3}, 0\right)$ are two equilibrium points, $(0,0)$ is a saddle point. When $c_4 = 1$, $\eta_1 = -3$, $\eta_2 = 0$, $\left(\sqrt{3}, 0\right)$, $\left(-\sqrt{3}, 0\right)$ are two saddle points, $(0,0)$ is an equilibrium point. We can see in Figs.3 and Figs.4, whether $c_4 > 0$ or $c_4 < 0$, the red closed curve represents the nonlinear periodic trajectories and the blue track indicates that it is the nonlinear homoclinic trajectories, and they respectively proved the existence of periodic and bell-shaped solitary solutions. However, the black trace in Fig.3 is depicted the supernonlinear periodic trajectories.

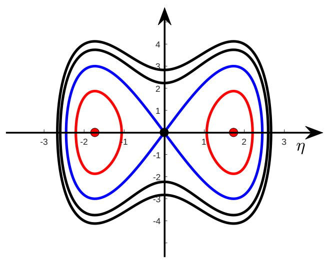

Figure 3. Corresponding phase portrait of Scenario 4, when $c_4 = -1$.

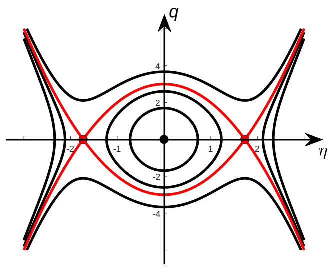

Figure 4. Corresponding phase portrait of Scenario 4, when $c_4 = -1$.

§4 Exact chirped solutions

In this section, we discussed the exact chirped solutions. Setting $s = \left(\frac{b_3}{2}\right)^{\frac{1}{4}} \kappa$, we reduce Eq.(10) to Eq.(17)

$$\left(\rho^{'}\right)^2 = \varepsilon \left(s^4 + l_1 s^2 + l_2 s + l_3\right) = G\left(s\right), \tag{17}$$

where

$$\begin{aligned}
&\varepsilon = \pm 1,\\
&l_1 = \left(\tfrac{b_3}{2}\right)^{-\frac{1}{2}} \tfrac{3b_1 b_3 - b_2^2}{3b_3},\\
&l_2 = \left(\tfrac{b_3}{2}\right)^{-\frac{1}{4}} \tfrac{4b_3^2 + 12b_1 b_2 b_3 + 36 b_3^2 b_0}{18 b_3^2},\\
&l_3 = c_1.
\end{aligned} \tag{18}$$

Simplify Eq.(17) to the integral form

$$\pm(\xi - \xi_0) = \int \frac{ds}{\sqrt{G(s)}}. \tag{19}$$

By the complete discrimination for polynomial method, we divide Eq.(12) into nine cases, and we obtain all chirped solutions for Eq.(1). According to the quartic polynomial discriminant system

$$\begin{aligned}
&D_1 = 4,\\
&D_2 = -l_1,\\
&D_3 = 8l_3 l_1 - 2l_1^3 - 9l_2,\\
&D_4 = 4l_1^4 l_3 - l_1^3 l_2^2 + 36 l_1 l_3 l_2^2 - 32 l_1^2 l_3^2 - \tfrac{27}{4} l_2^4 + 64 l_3^3,\\
&E_2 = 9l_1^2 - 32 l_1 l_3.
\end{aligned} \tag{20}$$

Then we analyse the roots of $G(s)$ to classify the solutions of Eq.(1).

State 1. When $D_2 < 0, D_3 = 0, D_4 = 0$, then $G(s) = [(s-\alpha)^2 + \beta^2]^2$, we have

$$h_1 = \left\{ \left(\frac{b_3}{2}\right)^{-\frac{1}{4}} \{\beta \tan[\beta(\zeta - \zeta_0)] + \alpha\} - \frac{b_2}{2b_3} \right\} e^{i(\chi(\xi) - kx)}. \tag{21}$$

This is a singular periodic pattern with an infinite number of discontinuities.

State 2.When $D_2 = 0, D_3 = 0, D_4 = 0$, then $G(s) = s^4$, we have

$$h_2 = \left\{ -\left(\frac{b_3}{2}\right)^{-\frac{1}{4}} (\zeta - \zeta_0)^{-1} - \frac{b_2}{2b_3} \right\} e^{i(\chi(\xi) - kx)}. \tag{22}$$

This is the singular rational pattern with discontinuity points.

State 3.When $D_2 > 0, D_3 = 0, D_4 = 0, E_2 > 0$, then $G(s) = (s-\alpha)^2(s-\beta)^2$, $\alpha > \beta$.

If $s > \alpha$ or $s < \beta$, we have

$$h_3 = \left\{ \left(\frac{b_3}{2}\right)^{-\frac{1}{4}} \left\{ \frac{\beta - \alpha}{2} [\coth\left[\frac{\alpha - \beta}{2}(\zeta - \zeta_0)\right] - 1] + \beta \right\} - \frac{b_2}{2b_3} \right\} e^{i(\chi(\xi) - kx)}, \tag{23}$$

if $\beta < s < \alpha$, we have

$$h_4 = \left\{ \left(\frac{b_3}{2}\right)^{-\frac{1}{4}} \left\{ \frac{\beta - \alpha}{2} [\tanh\left[\frac{\alpha - \beta}{2}(\zeta - \zeta_0)\right] - 1] + \beta \right\} - \frac{b_2}{2b_3} \right\} e^{i(\chi(\xi) - kx)}. \tag{24}$$

These are two solitary wave patterns.

State 4. when $D_2 > 0, D_3 > 0, D_4 = 0$, then $G(s) = \varepsilon(s-\alpha)^2(s-\beta)(s-\gamma)$, $\beta > \gamma$.

If $\varepsilon = 1$, $\alpha > \beta$ and $s > \beta$, the solution comes out as

$$h_5 = \left\{ \left(\tfrac{b_3}{2}\right)^{-\frac{1}{4}} \frac{\beta(\alpha-\gamma) + \gamma(\alpha-\beta)\coth^2 \frac{(\zeta-\zeta_0)\sqrt{(\alpha-\gamma)(\alpha-\beta)}}{2}}{(\alpha-\gamma) - (\alpha-\beta)\coth^2 \frac{(\zeta-\zeta_0)\sqrt{(\alpha-\gamma)(\alpha-\beta)}}{2}} - \frac{b_2}{2b_3} \right\} e^{i(\chi(\xi) - kx)}, \tag{25}$$

in this condition $\alpha > \beta > \gamma$ and $\alpha < \beta < \gamma$ have the same solutions.

If $\gamma < \alpha < \beta$, the solution comes out as

$$h_6 = \left\{ \left(\frac{b_3}{2}\right)^{-\frac{1}{4}} \frac{\gamma(\beta-\alpha)\tan^2\frac{(\zeta-\zeta_0)\sqrt{(\alpha-\gamma)(\beta-\alpha)}}{2}}{(\beta-\alpha)\tan^2\frac{(\zeta-\zeta_0)\sqrt{(\alpha-\gamma)(\beta-\alpha)}}{2}-(\alpha-\gamma)} - \frac{b_2}{2b_3} \right\} e^{i(\chi(\xi)-kx)}. \tag{26}$$

If $\varepsilon = -1$, $\alpha > \beta > \gamma$ or $\beta > \gamma > \alpha$, the solution comes out as

$$h_7 = \left\{ \left(\frac{b_3}{2}\right)^{-\frac{1}{4}} \frac{\beta(\gamma-\alpha)+\gamma(\beta-\alpha)\tan^2\frac{(\zeta-\zeta_0)\sqrt{(\gamma-\alpha)(\beta-\alpha)}}{2}}{(\beta-\alpha)\tan^2\frac{(\zeta-\zeta_0)\sqrt{(\gamma-\alpha)(\beta-\alpha)}}{2}+(\gamma-\alpha)} - \frac{b_2}{2b_3} \right\} e^{i(\chi(\xi)-kx)}, \tag{27}$$

if $\beta > \alpha > \gamma$, the solutions come out as

$$h_8 = \left\{ \left(\frac{b_3}{2}\right)^{-\frac{1}{4}} \frac{\beta(\alpha-\gamma)+\gamma(\beta-\alpha)\coth^2\frac{(\zeta-\zeta_0)\sqrt{(\alpha-\gamma)(\beta-\alpha)}}{2}}{(\beta-\alpha)\coth^2\frac{(\zeta-\zeta_0)\sqrt{(\alpha-\gamma)(\beta-\alpha)}}{2}+(\alpha-\gamma)} - \frac{b_2}{2b_3} \right\} e^{i(\chi(\xi)-kx)}, \tag{28}$$

$$h_9 = \left\{ \left(\frac{b_3}{2}\right)^{-\frac{1}{4}} \frac{\beta(\alpha-\gamma)+\gamma(\beta-\alpha)\tanh^2\frac{(\zeta-\zeta_0)\sqrt{(\alpha-\gamma)(\beta-\alpha)}}{2}}{(\beta-\alpha)\tanh^2\frac{(\zeta-\zeta_0)\sqrt{(\alpha-\gamma)(\beta-\alpha)}}{2}+(\alpha-\gamma)} - \frac{b_2}{2b_3} \right\} e^{i(\chi(\xi)-kx)}. \tag{29}$$

These are two solitary wave patterns and a singular periodic pattern.

State 5. When $D_2 > 0, D_3 = 0, D_4 = 0, E_2 = 0$, then $G(s) = \varepsilon(s-\alpha)^3(s-\beta)$.

If $\varepsilon = 1$, $s > \alpha, s > \beta$ or $s < \alpha, s < \beta$, the solution turns into

$$h_{10} = \left\{ \left(\frac{b_3}{2}\right)^{-\frac{1}{4}} \left[\alpha + \frac{4(\alpha-\beta)}{(\zeta-\zeta_0)^2(\beta-\alpha)^2-4}\right] - \frac{b_2}{2b_3} \right\} e^{i(\chi(\xi)-kx)}. \tag{30}$$

If $\varepsilon = -1$, $s > \alpha, s < \beta$ or $s < \alpha, s > \beta$, the solution turns into

$$h_{11} = \left\{ \left(\frac{b_3}{2}\right)^{-\frac{1}{4}} \left[\alpha - \frac{4(\alpha-\beta)}{(\zeta-\zeta_0)^2(\beta-\alpha)^2+4}\right] - \frac{b_2}{2b_3} \right\} e^{i(\chi(\xi)-kx)}. \tag{31}$$

This is a rational singular pattern.

State 6. When $D_2D_3 < 0, D_4 = 0$, then $G(s) = (s-\alpha)^2[(s-\beta)^2+\gamma^2]$, we have

$$h_{12} = \left\{ \left(\frac{b_3}{2}\right)^{-\frac{1}{4}} \left[\frac{e^{\pm\left((\zeta-\zeta_0)\sqrt{(\beta-\alpha)^2+\gamma^2}\right)}-\gamma+(2-\gamma)\sqrt{(\beta-\alpha)^2+\gamma^2}}{\left[e^{\pm\left((\zeta-\zeta_0)\sqrt{(\beta-\alpha)^2+\gamma^2}\right)}-\gamma\right]^2-1}\right] - \frac{b_2}{2b_3} \right\} e^{i(\chi(\xi)-kx)}. \tag{32}$$

This is a solitary wave solution.

State 7. When $D_4 > 0, D_3 > 0, D_1 > 0$, then $G(s) = \varepsilon(s-\alpha_1)(s-\alpha_2)(s-\alpha_3)(s-\alpha_4)$, $\alpha_1 > \alpha_2 > \alpha_3 > \alpha_4$.

If $\varepsilon = 1$, $\alpha_3 < s < \alpha_2$, the solution shapes up as

$$h_{13} = \left\{ \left(\frac{b_3}{2}\right)^{-\frac{1}{4}} \frac{\alpha_4(\alpha_2-\alpha_3)\,\mathrm{sn}^2[\frac{(\zeta-\zeta_0)\sqrt{(\alpha_1-\alpha_3)(\alpha_2-\alpha_4)}}{2},n_1]-\alpha_3(\alpha_2-\alpha_4)}{(\alpha_2-\alpha_3)\,\mathrm{sn}^2[\frac{(\zeta-\zeta_0)\sqrt{(\alpha_1-\alpha_3)(\alpha_2-\alpha_4)}}{2},n_1]-(\alpha_2-\alpha_4)} - \frac{b_2}{2b_3} \right\} e^{i(\chi(\xi)-kx)}, \tag{33}$$

if $s > \alpha_1$ and $s < \alpha_4$, the solution shapes up as

$$h_{14} = \left\{ \left(\frac{b_3}{2}\right)^{-\frac{1}{4}} \frac{\alpha_2(\alpha_1-\alpha_4)\,\mathrm{sn}^2[\frac{(\zeta-\zeta_0)\sqrt{(\alpha_1-\alpha_3)(\alpha_2-\alpha_4)}}{2},n_1]-\alpha_3(\alpha_2-\alpha_4)}{(\alpha_1-\alpha_4)\,\mathrm{sn}^2[\frac{(\zeta-\zeta_0)\sqrt{(\alpha_1-\alpha_3)(\alpha_2-\alpha_4)}}{2},n_1]-(\alpha_2-\alpha_4)} - \frac{b_2}{2b_3} \right\} e^{i(\chi(\xi)-kx)}, \tag{34}$$

where $n_1^2 = \frac{(\alpha_1-\alpha_4)(\alpha_2-\alpha_3)}{(\alpha_1-\alpha_3)(\alpha_2-\alpha_4)}$.

If $\varepsilon = -1$, $\alpha_2 < s < \alpha_1$, the solution shapes up as

$$h_{15} = \left\{ \left(\frac{b_3}{2}\right)^{-\frac{1}{4}} \frac{\alpha_3(\alpha_1-\alpha_2)\,\mathrm{sn}^2[\frac{(\zeta-\zeta_0)\sqrt{(\alpha_1-\alpha_3)(\alpha_2-\alpha_4)}}{2},n_2]-\alpha_2(\alpha_1-\alpha_3)}{(\alpha_1-\alpha_2)\,\mathrm{sn}^2[\frac{(\zeta-\zeta_0)\sqrt{(\alpha_1-\alpha_3)(\alpha_2-\alpha_4)}}{2},n_2]-(\alpha_1-\alpha_3)} - \frac{b_2}{2b_3} \right\} e^{i(\chi(\xi)-kx)}, \tag{35}$$

if $\alpha_4 < s < \alpha_3$, the solution shapes up as

$$h_{16} = \left\{ \left(\frac{b_3}{2}\right)^{-\frac{1}{4}} \frac{\alpha_1(\alpha_3-\alpha_4)\,\mathrm{sn}^2[\frac{(\zeta-\zeta_0)\sqrt{(\alpha_1-\alpha_3)(\alpha_2-\alpha_4)}}{2},n_2]-\alpha_4(\alpha_3-\alpha_1)}{(\alpha_3-\alpha_4)\,\mathrm{sn}^2[\frac{(\zeta-\zeta_0)\sqrt{(\alpha_1-\alpha_3)(\alpha_2-\alpha_4)}}{2},n_2]-(\alpha_3-\alpha_1)} - \frac{b_2}{2b_3} \right\} e^{i(\chi(\xi)-kx)}, \tag{36}$$

where $n_2^2 = \frac{(\alpha_1-\alpha_2)(\alpha_3-\alpha_4)}{(\alpha_1-\alpha_3)(\alpha_2-\alpha_4)}$.

These are double periodic patterns.

State 8. When $D_4 < 0, D_2D_3 \geq 0$, then $G(s) = \varepsilon(s-\alpha)(s-\beta)[(s-l)^2+k^2]$, $l, s > 0$, $\alpha > \beta$.

If $\varepsilon = 1$, the solution reads as

$$h_{17} = \left\{ \left(\tfrac{b_3}{2}\right)^{-\frac{1}{4}} \frac{p_1 \,\mathrm{cn}[\frac{(\zeta-\zeta_0)\sqrt{-2kn_3(\alpha-\beta)}}{2n_3n_4}, n_4]+p_2}{p_3 \,\mathrm{cn}[\frac{(\zeta-\zeta_0)\sqrt{-2kn_3(\alpha-\beta)}}{2n_3n_4}, n_4]+p_4} - \frac{b_2}{2b_3} \right\} e^{i(\chi(\xi)-kx)}, \tag{37}$$

If $\varepsilon = -1$, the solution read as

$$h_{18} = \left\{ \left(\tfrac{b_3}{2}\right)^{-\frac{1}{4}} \frac{p_1 \,\mathrm{cn}[\frac{(\zeta-\zeta_0)\sqrt{2kn_3(\alpha-\beta)}}{2n_3n_4}, n_4]+p_2}{p_3 cn[\frac{(\zeta-\zeta_0)\sqrt{2kn_3(\alpha-\beta)}}{2n_3n_4}, n_4]+p_4} - \frac{b_2}{2b_3} \right\} e^{i(\chi(\xi)-kx)}, \tag{38}$$

where

$$\begin{aligned} p_1 &= \frac{1}{2}(\alpha+\beta)p_3 - \frac{1}{2}(\alpha-\beta)p_4, \\ p_2 &= \frac{1}{2}(\alpha+\beta)p_4 - \frac{1}{2}(\alpha-\beta)p_3, \\ p_3 &= \alpha - l - \frac{k}{n_3}, \\ p_4 &= \alpha - l - kn_3, \\ E_1 &= \frac{k^2(\alpha-l)(\beta-l)}{k(\alpha-\beta)}, \\ n_3 &= E_1 \pm \sqrt{E_1^2+1}. \end{aligned} \tag{39}$$

These are double periodic patterns.

State 9.When $D_4 > 0, D_2D_3 \leq 0$, then $G(s) = [(s-\alpha_1)^2+{\beta_1}^2][(s-\alpha_2)^2+{\beta_2}^2]$, $\beta_1 \geq \beta_2 > 0$, the solution evolves as

$$h_{19} = \left\{ \left(\tfrac{b_3}{2}\right)^{-\frac{1}{4}} \frac{p_1 \,\mathrm{sn}[\gamma(\zeta-\zeta_0), n_5]+p_2 \,\mathrm{cn}[\gamma(\zeta-\zeta_0), n_5]}{p_3 \,\mathrm{sn}[\gamma(\zeta-\zeta_0), n_5]+p_4 \,\mathrm{cn}[\gamma(\zeta-\zeta_0), n_5]} - \frac{b_2}{2b_3} \right\} e^{i(\chi(\xi)-kx)}, \tag{40}$$

where

$$\begin{aligned} p_1 &= \alpha_1 p_1 + \beta_1 p_4, \\ p_2 &= \alpha_1 p_4 - \beta_1 p_3, \\ p_3 &= -\beta_1 - \frac{\beta_2}{n_1}, \\ p_4 &= \alpha_1 - \alpha_2, \\ E_3 &= \frac{(\alpha_1-\alpha_2)^2+\beta_1^2+\beta_2^2}{2\beta_1\beta_2}, \\ n_6 &= F_3 + \sqrt{F_3^2-1}, \\ n_5^2 &= \frac{n_6^2-1}{n_6^2}. \end{aligned} \tag{41}$$

This is a double periodic pattern.

§5 Typical Case Study

The solutions obtained above can be expressed in terms of specific parameters. Graphical representation of the motion of some results in order to facilitate the recognition of the physical phenomena of this nonlinear model. To save space, we only give a few typical cases.

Family 1. Singular solution

Making $\alpha = 2$, $\beta = -1$, $\gamma = -3$, $u = 2$, $k = \frac{2}{5}$ $t = 1$, $b_3 = 2$, $b_2 = 1$, then

$$h_6 = \left\{ \frac{-9\left(\tan\left[\frac{\sqrt{15}(1+2x)}{2}\right]\right)^2}{-3\left(\tan\left[\frac{\sqrt{15}(1+2x)}{2}\right]\right)^2 - 5} - \frac{1}{4} \right\} e^{i\left(\chi(\xi) - \frac{2}{5}x\right)}. \tag{42}$$

This is a singular rational solution and the $3D$ and $2D$ diagrams of the module of h_6 are shown in Figs.5 and 6.

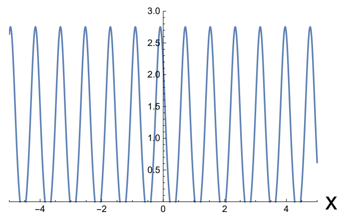

Figure 5. The $2D$ graph of $|h_6|$.

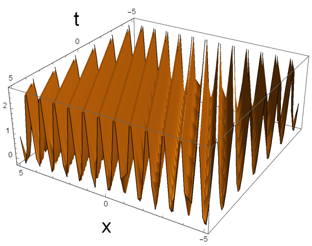

Figure 6. The $3D$ graph of $|h_6|$.

Family 2. Solitary wave solution

Making $\alpha = 1$, $\beta = -1$, $u = 2$, $t = 1$, $k = \frac{2}{5}$, $b_3 = 2$, $b_2 = 1$, then

$$h_3 = \left\{ -\tanh\left[\frac{1+2x}{2}\right] - \frac{1}{4} \right\} e^{i\left(\chi(\xi) - \frac{2}{5}x\right)}. \tag{43}$$

This is a solitary wave solution and the representation of the module of h_3 are shown in Figs.7 and 8.

Family 3. Double periodic solution

Making $\alpha_1 = 2$, $\alpha_2 = 1$, $\alpha_3 = -1$, $\alpha_4 = -2$, $u = 2$, $t = 1$, $k = \frac{2}{5}$, $b_3 = 2$, $b_2 = 1$, $n_1 = \frac{2\sqrt{2}}{3}$, then

$$h_{13} = \left\{ \frac{-4\,\mathrm{sn}^2\left[\frac{3}{2}(1+2x), \frac{2\sqrt{2}}{3}\right] + 3}{2\,\mathrm{sn}^2\left[\frac{3}{2}(1+2x), \frac{2\sqrt{2}}{3}\right] - 3} - \frac{1}{4} \right\} e^{i\left(\chi(\xi) - \frac{2}{5}x\right)}. \tag{44}$$

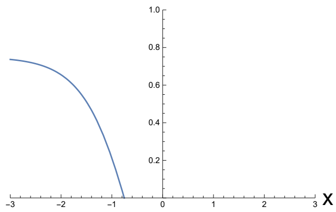

Figure 7. The $2D$ graph of $|h_3|$.

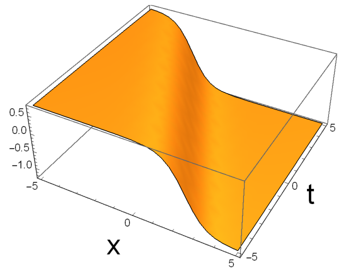

Figure 8. The $3D$ graph of $|h_3|$.

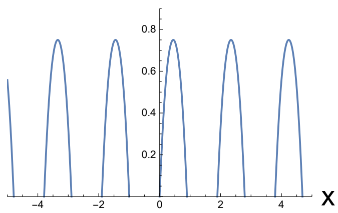

Figure 9. The $2D$ graph of $|h_{13}|$.

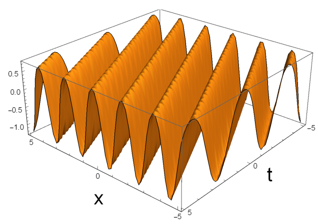

Figure 10. The $3D$ graph of $|h_{13}|$.

This is a double periodic solution and the $3D$ and $2D$ diagrams of the module of h_{13} are shown in Figs.9 and 10.

§6 Conclusion

In this paper, the resonant nonlinear Schrödinger equation with quadratic-cubic nonlinearity is solved by using the trial equation method and the complete discrimination for polynomial method. These methods can only achieve single traveling wave solutions, not obtain multiple solitary solutions. Therefore, researchers have to continue to study. We use the bifurcation method to prove the existence of different types of solutions, and classify these solutions into three types : singular solutions, solitary wave solutions, and double periodic solutions. We also give some implemented solutions in $2D$ and $3D$, and different parameters are chosen to obtain solutions presenting the characteristics of an optical soliton and could be used in telecommunications, industry, the design of new waveguides, as well as in the choice of incident pulses that would optimize the transmission of information. These solutions ensure all chirped solutions for optical solitons in magneto-optical waveguides, allowing the observation of the rich propagation pattern of the light waves in the fiber. And chirped solutions help to solve the problem of solitary dynamics in magneto-optical waveguides, which also have important applications in physical and applied sciences.

Declarations

Conflict of interest The authors declare no conflict of interest.

References

[1] M Gitterman. *Introduction to nonlinear science*, Journal of Statistical Physics, 1996, 83(5): 1261-1262.

[2] V E Zakharov. *Collapse of Langmuir waves*, Journal of Experimental and Theoretical Physics, 1972, 35(5): 908-914.

[3] C Hamner, J J Chang, P Engels, et al. *Generation of dark-bright soliton trains in superfluid-superfluid counterflow*, Physical Review Letters, 2011, 106(6): 065302.

[4] A H Khater, D K Callebaut, M A Helal, et al. *Variational method for the nonlinear dynamics of an elliptic magnetic stagnation line*, The European Physical Journal D, 2006, 39: 237-245.

[5] A R Seadawy. *New exact solutions for the KdV equation with higher order nonlinearity by using the variational method*, Computers and Mathematics with Applications, 2011, 62(10): 3741-3755.

[6] H Akiyama, F Tappert. *Transmission of stationary nonlinear optical pulses in dispersive dielectric fibers. II. Normal dispersion*, Applied Physics Letters, 1973, 23(4): 171-172.

[7] Y J Kodama. *Optical solitons in a monomode fiber*, Journal of Statistical Physics, 1985, 39: 597-614.

[8] R C Yang, R Y Hao, L Li, et al. *Dark soliton solution for higher-order nonlinear Schrödinger equation with variable coefficients*, Optics communications, 2004, 242(1-3): 285-293.

[9] J Fujioka, E Cortés, R Pérez-Pascual, et al. *Chaotic solitons in the quadratic-cubic nonlinear Schrödinger equation under nonlinearity management*, Chaos: An Interdisciplinary Journal of Nonlinear Science, 2011, 21(3), DOI: 10.1063/1.3629985.

[10] H Triki, K Porsezian, A Choudhuri, et al. *W-shaped, bright and kink solitons in the quadratic-cubic nonlinear Schrödinger equation with time and space modulated nonlinearities and potentials*, Journal of Modern Optics, 2017, 64(14): 1368-1376.

[11] R Pal, H Kaur, A Goyal, et al. *Dynamics of Jacobi elliptic and soliton solutions for the modified quadratic-cubic nonlinear Schrödinger equation*, Journal of Modern Optics, 2019, 66(5): 571-579.

[12] A R Seadawy, S T Rizvi, B Mustafa, et al. *Chirped periodic waves for an cubic quintic nonlinear Schrödinger equation with self steepening and higher order nonlinearities*, Chaos, Solitons and Fractals, 2022, 156: 111804.

[13] J Chai, B Tian, H L Zhen, et al. *Conservation laws, bilinear forms and solitons for a fifth-order nonlinear Schrödinger equation for the attosecond pulses in an optical fiber*, Annals of Physics, 2015, 359: 371-384.

[14] M Justin, M B Hubert, G Betchewe, et al. *Chirped solitons in derivative nonlinear Schrödinger equation*, Chaos, Solitons and Fractals, 2018, 107: 49-54.

[15] S T R Rizvi, A R Seadawy, S Ahmed, et al. *Study of multiple lump and rogue waves to the generalized unstable space time fractional nonlinear Schrödinger equation*, Chaos, Solitons and Fractals, 2021, 151: 111251.

[16] A Biswas, M Z Ullah, Q Zhou, et al. *Resonant optical solitons with quadratic-cubic nonlinearity by semi-inverse variational principle*, Optik, 2017, 145: 18-21.

[17] A R Seadawy, D Lu, N Nasreen, et al. *Structure of optical solitons of resonant Schrödinger equation with quadratic-cubic nonlinearity and modulation instability analysis*, Physica A: Statistical Mechanics and its Applications, 2019, 534: 122155.

[18] S T R Rizvi, A R Seadawy, U Raza. *Some advanced chirped pulses for generalized mixed nonlinear Schrödinger dynamical equation*, Chaos, Solitons and Fractals, 2022, 163: 112575.

[19] F Wang, J Liu, L Liu, et al. *Quantitative non-destructive evaluation of CFRP delamination defect using laser induced chirp-pulsed radar photothermal tomography*, Optics and Lasers in Engineering, 2022, 149: 106830.

[20] S R Konda, V R Soma, R A Ganeev, et al. *Third-order optical nonlinearities and high-order harmonics generation in Ni-doped* $CsPbBr_3$ *nanocrystals using single-and two-color chirped pulses*, Journal of Materials Science, 2022, 57(5): 3468-3485.

[21] S Yang. *Chirped envelope solutions of the Triki-Biswas equation*, Optik, 2021, 244: 167542.

[22] H Triki, Q Zhou, W Liu, et al. *Chirped optical soliton propagation in birefringent fibers modeled by coupled Fokas-Lenells system*, Chaos, Solitons and Fractals, 2022, 155: 111751.

[23] H Triki, Q Zhou, A Biswas, et al. *Chirped optical solitons having polynomial law of nonlinear refractive index with self-steepening and nonlinear dispersion*, Physics Letters A, 2021, 417: 127698.

[24] H Triki, A Benlalli, Q Zhou, et al. *Formation of chirped kink similaritons in non-Kerr media with varying Raman effect*, Results in Physics, 2021, 26: 104381.

[25] A Biswas, M Ekici, A Sonmezoglu, et al. *Sub-pico-second chirped optical solitons in mono-mode Fibers with Kaup-Newell equation by extended trial function method*, Optik, 2018, 168: 208-216.

[26] S Arshed, G Akram, M Sadaf, et al. *Optical soliton solutions of perturbed nonlinear Schrödinger equation with parabolic law nonlinearity*, Optical and Quantum Electronics, 2024, 56(1): 50.

[27] G Akram, M Sadaf, I Zainab. *Effect of a new local derivative on space-time fractional nonlinear Schrödinger equation and its stability analysis*, Optical and Quantum Electronics, 2023, 55(9): 834.

[28] S Arshed, G Akram, M Sadaf, et al. *A variety of structures of optical solitons for the nonlinear Schrödinger equation with generalized anti-cubic nonlinearity*, Optical and Quantum Electronics, 2023, 55(6): 542.

[29] M Sadaf, S Arshed, G Akram, et al. *A variety of solitary waves solutions for the modified nonlinear Schrödinger equation with conformable fractional derivative*, Optical and Quantum Electronics, 2023, 55(4): 372.

[30] A Mecelti, H Triki, F Azzouzi, et al. *New chirped gray and kink self-similar waves in presence of quintic nonlinearity and self-steepening effect*, Physics Letters A, 2022, 437: 128104.

[31] Q Zhou, H Triki, J Xu, et al. *Perturbation of chirped localized waves in a dual-power law nonlinear medium*, Chaos, Solitons and Fractals, 2022, 160: 112198.

[32] S Arshed, G Akram, M Sadaf, et al. *Extraction of new exact solutions of the resonant fractional nonlinear Schrödinger equation via two integrating techniques*, Optical and Quantum Electronics, 2022, 54(12): 799.

[33] H Bulut, A S Tukur, M B Haci. *Optical solitons to the resonant nonlinear Schrödinger equation with both spatio-temporal and inter-modal dispersions under Kerr law nonlinearity*, Optik, 2018, 163: 49-55.

[34] H Rezazadeh, N Ullah, L Akinyemi, et al. *Optical soliton solutions of the generalized non-autonomous nonlinear Schrödinger equations by the new Kudryashov's method*, Results in Physics, 2021, 24: 104179.

[35] M Inc, A I Aliyu, A Yusuf, et al. *Optical solitons to the resonance nonlinear Schrödinger equation by Sine-Gordon equation method*, Superlattices and Microstructures, 2018, 113: 541-549.

[36] M A Akbar, L Akinyemi, S W Yao, et al. *Soliton solutions to the Boussinesq equation through sine-Gordon method and Kudryashov method*, Results in Physics, 2021, 25: 104228.

[37] L Akinyemi, H Rezazadeh, S W Yao,et al. *Nonlinear dispersion in parabolic law medium and its optical solitons*, Results in Physics, 2021, 26: 104411.

[38] H Ahmad, T A Khan, I Ahmad, et al. *A new analyzing technique for nonlinear time fractional Cauchy reaction-diffusion model equations*, Results in Physics, 2020, 19: 103462.

[39] H Ahmad, A Akgül, T A Khan, et al. *New perspective on the conventional solutions of the nonlinear time-fractional partial differential equations*, Complexity, 2020, 2020: 1-10.

[40] H Ahmad, T A Khan. *Variational iteration algorithm-I with an auxiliary parameter for wave-like vibration equations*, Journal of Low Frequency Noise, Vibration and Active Control, 2019, 38(3-4): 1113-1124.

[41] H Ahmad, T A Khan, C Cesarano. *Numerical solutions of coupled Burgers' equations*, Axioms, 2019, 8(4): 119.

[42] H Ahmad, T A Khan, P S Stanimirovi, et al. *Modified variational iteration algorithm-II: convergence and applications to diffusion models*, Complexity, 2020, 2020: 1-14.

[43] H Ahmad, A R Seadawy, T A Khan. *Study on numerical solution of dispersive water wave phenomena by using a reliable modification of variational iteration algorithm*, Mathematics and Computers in Simulation, 2020, 177: 13-23.

[44] O Bazighifan, H Ahmad, S W Yao. *New oscillation criteria for advanced differential equations of fourth order*, Mathematics, 2020, 8(5): 728.

[45] I Ahmad, H Ahmad, M Inc, et al. *Application of local meshless method for the solution of two term time fractional-order multi-dimensional PDE arising in heat and mass transfer*, Thermal Science, 2020, 24(Suppl.1): 95-105.

[46] M Inc, M N Khan, I Ahmad, et al. *Analysing time-fractional exotic options via efficient local meshless method*, Results in Physics, 2020, 19: 103385.

[47] H Ahmad, M N Alam, M Omri. *New computational results for a prototype of an excitable system*, Results in Physics, 2021, 28: 104666.

[48] C S Liu. *Trial equation method and its applications to nonlinear evolution equations*, Acta Physica Sinica, 2005, 54(6): 2505-2509.

[49] C S Liu. *Trial equation method based on symmetry and applications to nonlinear equations arising in mathematical physics*, Foundations of Physics, 2011, 41: 793-804.

[50] C S Liu. *Using trial equation method to solve the exact solutions for two kinds of KdV equations with variable coefficients*, Acta Physica Sinica, 2005, 54(10): 4506-4510.

[51] C S Liu. *Trial equation method for nonlinear evolution equations with rank inhomogeneous: mathematical discussions and applications*, Communications In Theoretical Physics, 2006, 45(2): 219-223.

[52] C S Liu. *Exponential function rational expansion method for nonlinear differential-difference equations*, Chaos, Solitons and Fractals, 2009, 40(2): 708-716.

[53] C S Liu. *Exact Traveling Wave Solutions for a Kind of Generalized Ginzburg-Landau Equation*, Communications in Theoretical Physics, 2005, 43(5): 787-790.

[54] C S Liu. *Applications of complete discrimination system for polynomial for classifications of traveling wave solutions to nonlinear differential equations*, Computer Physics Communications, 2010, 181(2): 317-324.

[55] J X Tang, X Su. *Traveling wave solutions, dynamic properties and chaotic behaviors of Schrödinger equation in magneto-optic waveguide with anti-cubic nonlinearity*, Results in Physics, 2023, 54: 107106.

Department of Mathematics, Northeast Petroleum University, Daqing 163318, China.

Email: florine0222@163.com